Manuscript Number: STRUCTURES-D-20-00206R1

Title: Re-tuning an off-tuned tuned mass damper by adjusting temperature of shape memory alloy: exposed to wind action

Article Type: Research Paper

Keywords: Shape memory alloy; wind action; tuned mass damper; retune; off-tuning

Corresponding Author: Dr. Wen-Shao Chang,

Corresponding Author's Institution:

First Author: Haoyu Huang

Order of Authors: Haoyu Huang; Wen-Shao Chang

Abstract: To reduce the wind-induced vibration of building structures, tuned mass damper (TMD) is a widely used approach. However, the off-tune of TMD can cause larger excessive vibration to the structure. In this study, shape memory alloy (SMA) is employed in TMD for retuning. At first, the dynamic properties of SMA-based TMD were characterised by free vibration at between -40℃ and 65℃. It is found the stiffness increased and damping reduced with rising temperature. Next, the SMA-based TMD was applied to a steel frame structure under wind excitations. The wind action was generated by autoregressive models method and input by a shaking table. The results present the wind-induced vibration can be attenuated effectively by installing a SMA-based TMD. By changing the main structural mass, the TMD was easy to be off-tuned and the structural response was increased. By means of cooling SMA to retune the TMD, the response of the system can be reduced effectively. However, the effect of heating SMA was relatively small. The increase of damping capacity by combing multiple SMA bars and the applications of SMAs with higher phase transformation temperatures are important to be further investigated in TMD, so as to improve the effectiveness of heating SMA.

Response to Reviewers: See attached

Re-tuning an off-tuned tuned mass damper by adjusting temperature of shape memory alloy: exposed to wind action

Haoyu Huang

BEng, PhD

Lecturer, Beijing Key Lab of Earthquake Engineering and Structural Retrofit, the Key Laboratory of Urban Security and Disaster Engineering of Ministry of Education, Beijing University of Technology, Beijing 100124, China

ORCID: https://orcid.org/0000-0003-4216-4516

Wen-Shao Chang*

BSArch, MSArch, PhD, FHEA

Senior Lecturer, School of Architecture, University of Sheffield, Sheffield, UK

ORCID: https://orcid.org/0000-0002-2218-001X

* Corresponding author, w.chang@sheffield.ac.uk

Number of words in main text and tables: 5753

Number of figures: 13

Abstract

To reduce the wind-induced vibration of building structures, tuned mass damper (TMD) is a widely used approach. However, the off-tune of TMD can cause larger excessive vibration to the structure. In this study, shape memory alloy (SMA) is employed in TMD for retuning. At first, the dynamic properties of SMA-based TMD were characterised by free vibration at between -40℃ and 65℃. It is found the stiffness increased and damping reduced with rising temperature. Next, the SMA-based TMD was applied to a steel frame structure under wind excitations. The wind action was generated by autoregressive models method and input by a shaking table. The results present the wind-induced vibration can be attenuated effectively by installing a SMA-based TMD. By changing the main structural mass, the TMD was easy to be off-tuned and the structural response was increased. By means of cooling SMA to retune the TMD, the response of the system can be reduced effectively. However, the effect of heating SMA was relatively small. The increase of damping capacity by combing multiple SMA bars and the applications of SMAs with higher phase transformation temperatures are important to be further investigated in TMD, so as to improve the effectiveness of heating SMA.

Keywords

Shape memory alloy; wind action; tuned mass damper; retune; off-tuning

1. Introduction

Buildings can be affected by wind-induced vibration, and the reliability of structures and comfort level of residents are issues which must be addressed by designers. To reduce the vibration, tuned mass damper (TMD) is a frequently used approach, and is less-complex and space-saving compared with other damping systems. In recent years, TMD is developed fast and has been applied to Taipei 101 in Taipei, the Bloomberg Tower in New York, the Sydney Tower in Sydney, the CN Tower in Toronto and the John Hancock Tower in Boston. The basic principle of TMD is that its natural frequency can be tuned to a particular range, so the damper can resonate with the structure relatively (Connor and Laflamme, 2014). The relative motion of TMD is a way of outputting energy, thus the energy input in the structure can be dissipated and the vibration can be mitigated. TMD can be simulated by consisting of mass (m_2), spring (k_2) and damper (c_2) as shown in Figure 1 (a). TMD is usually installed in the location where the motion is the greatest such as the top floor (Irwin et al., 2008). Figure 1 (b) presents the idealisation of TMD system into a 2-degree-of-freedom model, where m_1, k_1 and c_1 denote the mass, stiffness and damping coefficient of main structure.

The natural frequency of TMD is determined by Equation (1):

$$f_2 = \frac{1}{2\pi}\sqrt{\frac{k_2}{m_2}} \qquad (1)$$

where f_2 denotes the natural frequency of TMD, and k_2 and m_2 imply the stiffness and mass of TMD. The effectiveness of vibration control using TMD can be improved by controlling these parameters: mass ratio and natural frequency ratio between TMD and main structure as well as damping ratio of TMD. The optimal design of TMD parameters was studied, and classical designs can refer to Den Hartog (1956), Sadek et al. (1997), Tsai and Lin (1993) and Warburton (1982). As TMD is a passive vibration control approach, the drawback of using TMD is that TMD could be off-tuned when the main structural condition changes. For instance, the stiffness and mass of buildings usually vary due to climatic events, decoration, repair, and movement of people and facilities (Xue et al., 2009, Brincker et al., 2004). When the mass and stiffness of the main structure are changed, the tuned condition is influenced and the effectiveness of TMD is degraded (Huang et al., 2017). In off-tuned condition, the structural response subject to vibration may increase greatly (Huang et al., 2017), and the structural safety is threatened.

To overcome this drawback, semi-active TMD (Fisco and Adeli, 2011) is developed as an another passive vibration control approach. In semi-active TMD systems, actively adjustable springs, piezoelectric friction, shape memory alloy (SMA) and other techniques have been employed to adjust the natural frequency of TMD in order to retune it to an expected frequency range (Sun and LI, 2009, Jiang and Hanagan, 2006, Nagarajaiah and Sonmez, 2007). SMA is a smart material with particular thermomechanical properties, and is of potential to be applied to TMD. SMA has two phases: martensite and austenite. As seen in Figure 2 (a), the phase transformation depends on four temperatures: M_s, M_f, A_s and A_f which indicate the start and finish temperature of martensitic and austenitic transformation, respectively. In martensite when in-service temperature is below M_f, the loading behaviour is shape-memory effect, in which the residual strain can recover to the original point by external heating shown in Figure 2 (b). Martensite has been studied in reinforced concrete and masonry reparation (Soroushian et al., 2001, Indirli et al., 2001). When the working temperature is above A_f, SMA is austenitic; SMA is superelastic and its loading-unloading curve behaves self-centering as expressed in Figure 2 (c). In a whole, the change of in-service temperature can lead to the change of mechanical behaviours, and stiffness and damping ratio can be varied thereupon (Shaw and Kyriakides, 1995, Araya et al., 2008, Andrawes and DesRoches, 2007). Regarding to fatigue life of SMA, Torra et al. indicated SMA installed in civil structures is expected to withstand a large number of minor oscillations due to the actions of wind (Torra et al., 2009). Our study on SMA material characterisation presents SMA has long fatigue life under small strain level (Huang et al., 2020b). These properties of SMA create the possibility to apply to semi-active TMD.

In mechanical engineering domain, SMA-based tuned mass damper has been developed. Williams et al. (2002) and Aguiar et al. (2013) adjusted the stiffness of SMA by Joule heating so as to change the natural frequency of TMD. Savi et al. (2011), Elahinia et al. (2005) and Williams et al. (2005) conducted numerical studies to investigate the applications of SMA in tuneable mass damper. Most of studies used SMA wires for temperature control in TMD, and heating is mainly from electric current on SMA wires (Rustighi et al., 2005, Aguiar et al., 2013, Mani and Senthilkumar, 2015, Tiseo et al., 2010). Unlike mechanical engineering, effectiveness of using larger size like SMA bars in civil engineering needs to be concerned. Our feasibility study changed the natural frequency of a SMA bar-based TMD attached on a steel cantilever beam through heating and cooling, the excessive free vibration caused by off-tune was effectively attenuated (Huang et al., 2017). Huang and Chang (2018) presented the effectiveness of the SMA-based TMD in reducing the timber floor vibration. More studies regarding the applications of SMA bar to TMD subject to earthquake and wind excitations should be carried out.

The effectiveness of the semi-active TMD in reducing wind-induced structural response has been studied. Yang et al. (2001) investigated the performance of a semi-active magnetorheological TMD in a 76-storey building under wind loading, and considered it to be beneficial. Nagarajaiah and Varadarajan (2005) developed e new semi-active variable stiffness tuned mass damper to reduce the response of wind excited tall buildings. Kang et al. (2011) used a semi-active TMD in which both damping and stiffness can be variable, and the results showed this semi-active TMD could effectively control the vibration of a tall building subject to wind load. Concerning the free vibration testing of SMA-based TMD in our feasibility study (Huang et al., 2017), the vibration can be controlled by varying the natural frequency. It is important the effectiveness of the SMA-based TMD can be examined under wind excitation, as the wind contains wider frequency range unlike machine-induced vibration. To assess the performance of TMD under wind action, theoretical simulation is mostly used. In this study, a new experimental approach is developed, in which shaking table is used to simulate the wind action. Therefore, a theory of simulating wind action by shaking table is needed, so as to examine the effectiveness of TMD under the wind.

In this study, a SMA-based variable stiffness and damping TMD was designed and tested, and then applied to a steel frame structure subject to wind loading. By changing the supplementary mass on the main structure to trigger off-tuned situations, the retuning ability of SMA-based TMD was assessed by adjusting the working temperature. The excessive vibration from off-tune is aimed to be reduced by SMA temperature control.

2. Dynamic characterisation of the SMA-based TMD and main structural system by free vibration

In this study, a temperature controlled SMA-based TMD is aimed to be developed and applied to a steel frame structure to reduce the dynamic response subject to wind loading. Therefore, the dynamic properties of the TMD and steel frame structure need to be characterised. Moreover, the effect of temperature on dynamic properties of TMD should be examined. In this section, the variance of stiffness and equivalent viscous damping ratio of TMD under different temperature by free vibration testing are presented, and furthermore the characterisation of the main structure is illustrated.

2.1 Dynamic characterisation of the SMA-based TMD

SMA used in this study is a Cu-Al-Mn (Cu = 81.84%, Al = 7.43% and Mn = 10.73% by weight) SMA bar. The transformation temperatures M_s, M_f, A_s and A_f were tested by differential scanning calorimetry (DSC), and results show $M_s = -9$℃, $M_f = -25$℃, $A_s = -8$℃ and $A_f = 5$℃. In other word, under cooling process, SMA is martensitic when the in-service temperature is below -25℃. When SMA is heated, SMA completes transformation to austenite after 5℃. The material characterisation of Cu-Al-Mn SMA bars under dynamic bending was performed in our previous material study (Huang et al., 2020b). The material hysteresis, stiffness, damping ratio, and fatigue life were studied under strain levels of 0.5%, 1%, 2%, and 6%. The test results showed Cu-Al-Mn SMA has stable material properties along the dynamic loading and an adequate fatigue life. In this study, dynamic characterisation of SMA-based TMD was carried out at $-40, -20, 0, 19, 45,$ and 65℃, where 19℃ is the ambient temperature in laboratory. The the SMA cooling is conducted by spraying Tetrafluoroethane, and heating is implemented by wrapping energised carbon fibre.

In our feasibility studies, the SMA bar was attached to a beam horizontally with pre-stressed load (Huang et al., 2017). In this study, the SMA bar is placed vertically without pre-stress. The free vibration tests are same with our previous study investigating the effectiveness of SMA-based TMD exposed to earthquake excitations (Huang et al., 2020a). As shown in Figure 3 (a), the effective length of SMA bar is 280 mm, and the cross section was machined to 3×12 mm in order to facilitate the unidirectional vibration. As presented in Figure 3 (b), the bottom side of SMA bar was attached with a steel block of 6.4kg, and the top side was fixed rigidly. The free vibration tests were initiated by giving a 10mm displacement at the bottom at different in-service temperatures. The natural frequency and equivalent viscous damping ratio were computed using the linear-prediction singular-value decomposition-based matrix pencil (SVD-MP) method. This approach is able to deal with the approximation for complex exponentials and exhibits high precision in estimating the frequency and damping from measured data. Detailed descriptions can be found in Sarkar and Pereira (1995) and Zieliński and Duda (2011). The SVD-MP approach is based on Equations (2) and (3):

$$y(t) = x(t) + n(t) \approx \sum_{i=1}^{M} R_i \exp(s_i t) + n(t); 0 \leq t \leq T \tag{2}$$

where $y(t)$ is the observed time response, $x(t)$ is the signal, $n(t)$ is the noise in system, and R_i denotes the complex amplitudes. s_i is presented in Equation (3):

$$s_i = -\alpha_i + j\omega_i \tag{3}$$

117 where α_i and ω_i represent the damping factors and the angular frequencies, respectively, and

118 $j = \sqrt{-1}$. As shown in Equation (2), the objective of SVD-MP is to estimate the frequencies and

119 damping factors from the noise-contaminated data. Thus, solving the parameters is a non-linear

120 problem. According to the equation derivations in Sarkar and Pereira (1995), the matrix pencil is a

121 one-step process for solving a non-linear problem that is computationally efficient. Linear-prediction

122 singular-value decomposition provides a method for decomposing the eigenvectors when using the

123 matrix pencil.

124 The results show the natural frequency at 19°C is 1.68 Hz. Stiffness was therefore calculated from

125 natural frequency. Figure 4 shows the effect of temperature on stiffness and damping ratio. Stiffness

126 increases and damping ratio decreases with rising temperature from −40°C to 65°C. The change of

127 stiffness is dramatic between −20°C and 0°C while the damping ratio is sensitive to temperature

128 between −40°C and 0°C. As aforementioned about the phase transformation temperatures which

129 are from −25°C to 5°C, the mechanical properties are varied around this temperature range due to

130 the influence of the phase transformation between martensite and austenite. On the whole, the

131 stiffness and damping ratio can be adjusted for up to about 85% and 44% in the testing temperature

132 range, respectively, which presents the potential of using SMA in semi-active TMD.

133 2.2 Dynamic characterisation of main structure

134 The main structure used in this study is the same steel frame which was used in our previous study

135 investigating the performance subject to earthquake loadings as shown in Figure 5 (Huang et al.,

136 2020a). The steel frame is 1.2 m high and 0.6 m wide, and detailed dimensions can be seen in Figure

137 5 (b). The beam ends were not welded on the columns, and the column-beam connections were

138 built as hinge joints with three paralleled springs to facilitate the rotation. Therefore, the steel

139 framed structure is flexible in the horizontal direction. At the direction perpendicular to the vibration,

140 bracings were added. The detailed descriptions of the steel frame can be referred to Huang et al.

141 (2020a).

The dynamic characterisation of this steel frame with added mass of 10, 25, 30, 35 and 45 kg was done by free vibration. The free vibration was initiated by a shake with a displacement of 5mm from a shaking table shown in Figure 5 (a). The acceleration was measured by accelerometers for 1 minute. When the added mass at the top floor is 30 kg, the natural frequency of the steel frame is 1.78Hz. The optimal design method of TMD can be referred to Warburton (1982). There are two reasons why the Warburton (1982) method was selected as the optimal design method in this study. Firstly, the Warburton method is a classical analytical procedure for designing optimum parameters of TMD under various combinations of excitation and response, which is suitable for the civil engineering application employed in this study. The Warburton method has been widely cited and its effectiveness was demonstrated in previous studies by Hadi and Arfiadi (1998), Miguel et al. (2016) and Islam et al. (2018). Secondly, the Warburton method is a simplified analytical procedure and thus the semi-active vibration control in this study can be eased. By using Warburton (1982)'s optimal design theory presented in Equation (4) and (5):

$$f_{opt} = \sqrt{\frac{(1-\mu/2)}{1+\mu}} \tag{4}$$

$$\zeta_{opt} = \sqrt{\frac{\mu(1-\mu/4)}{4(1+\mu)(1-\mu/2)}} \tag{5}$$

The natural frequency of TMD should be near 1.66 Hz. In the Equation (4) and (5), μ represents the mass ratio between TMD and main structure, and f_{opt} and ζ_{opt} mean optimised natural frequency ratio and damping ratio. The natural frequency of the SMA-based TMD developed in this study is 1.68 Hz as aforementioned in 2.1, which is near the expected value 1.66 Hz. However, the damping ratio of SMA-based TMD is lower than the theoretical expected value calculated by Equation (5).

3. Wind input generation

To assess the effectiveness of the SMA-based TMD subject to wind excitation, the method utilised to simulate the wind action is illustrated in this section. In this study, a shaking table test is applied, which represents a new approach for modelling wind excitation.

3.1 Generation of fluctuating wind force time history

The wind action on a structure can be categorised into the average wind and fluctuating wind. The wind speed and direction of the average wind are constant over time, and it is dependent on the altitude. Fluctuating wind speed time history is a zero-mean Gaussian stochastic process and is characterised by the power spectrum and correlation functions. In this study, the wind action is modelled by fluctuating wind time history. The autoregressive models (AR) method is applied to this study for the purpose of generating fluctuating wind. Wind speed history over time in the AR method can be expressed by Equation (6) (Liang and Liu, 2012):

$$V(t) = \sum_{k=1}^{p} \Psi_k V(t - k\Delta t) + N(t) \tag{6}$$

where p is AR model order, Δt is the length of the time step, Ψ_k is the regression coefficient matrix for the AR model, $k = 1, 2, \cdots, p$ and $N(t)$ is the independent random process vector. Furthermore, Ψ_k can be derived from Equation (7):

$$R_v(j\Delta t) = \sum_{k=1}^{p} R_v[(j-k)\Delta t]\Psi_k \, , j = 1,2, \cdots p \tag{7}$$

where $R_v(j\Delta t)$ is correlation matrix, and it is expressed in Equation (8)

$$R_v(j\Delta t) = \int_0^{\infty} S_v(f) \cos(\omega \Delta t) \, d\omega \tag{8}$$

In this study, the Davenport power spectrum $S_v(f)$ (Davenport, 1961) is used for characterising the stochastic behaviours of fluctuating wind speed, which can be expressed by Equation (9):

$$S_v(f) = 4K\overline{v_{10}}^2 \frac{X^2}{f(1+X^2)^{4/3}} \tag{9}$$

where $S_v(f)$ describes the fluctuating wind velocity spectrum. $\overline{v_{10}}$ is the mean wind velocity at an altitude of 10 meters, $X = \frac{1200f}{\overline{v_{10}}}$, f is the frequency, and K is the surface resistance coefficient. Through the derivations in Equation (7), (8) and (9), Ψ_k can be computed.

To acquire $N(t)$:

$$N(t) = Ln(t) \tag{10}$$

$n(t)$ is a normal random process vector within (0,1) and the members in $n(t)$ are independent of each other. The mean value of $n(t)$ is 0, and the variance is 1. If the wind speed time history is required for M points in the space coordinates, L would be an M-triangle matrix, which can be decomposed from the M-matrix R_N by Cholesky decomposition, as shown in Equation (11). Furthermore, R_N can be solved by Equation (12).

$$R_N = LL^T \tag{11}$$

$$R_v(0) = \sum_{k=1}^{p} \Psi_k R_v(k\Delta t) + R_N \tag{12}$$

The relationship between fluctuating wind pressure and fluctuating wind speed is shown in Equation (13):

$$w(z,t) = \frac{1}{2}\rho[2\overline{v(z)}V(z,t) + v^2(z,t)] \tag{13}$$

where $\bar{v}$ is the mean wind speed at a height of z and ρ is the air density. $w(z,t)$ is the wind pressure at the height of z. Therefore, the wind force can be calculated by Equation (14), where the *Area* represents the area on the structure subject to wind action.

$$F(t) = w(z,t) \times Area \tag{14}$$

3.2 Derivation from wind force to ground motion

In this study, the wind motion acting on the structure is modelled by means of inputting ground motion using a shaking table. This is illustrated in Figure 6 (a) and (b), which present a forced vibration system and a base-excited vibration system of a single-degree-of-freedom model, respectively. The dynamic characterisations of forced vibration and base-excited vibration can be described by Equations (15) and (16), respectively. By equating the structural displacement *x* in these two systems, the ground motion *z* in Figure 6 (b) can be derived by the force *F* in Figure 6 (a).

$$m\ddot{x} = F - kx - c\dot{x} \tag{15}$$

$$m\ddot{x} = kz - kx + c\dot{z} - c\dot{x} \tag{16}$$

Through a combination of Equation (15) and (16), the ground motion $z(n)$ can be computed by applying the steps in the flow diagram shown in Figure 7. In Figure 7, n implies the serial number of each time step, and N is the total number of time steps. Figure 7 shows the ground motion computed by the theory demonstrated above, which will be used to model the fluctuating wind action applied via shaking table in the next section.

4. Performance of the structure with an off-tuned TMD subject to wind excitation

By varying the mass added on the structure, the natural frequency of the structure would be modified and, as a consequence, the TMD could become off-tuned. In this section, the structural response caused by TMD off-tuning under wind excitation is assessed.

4.1 Methods

The non-pre-stressed SMA-based TMD described in Section 2, as shown in Figure 3 (b), was installed on the steel framed structure as shown in Figure 5 vertically. The installation of the SMA-based TMD is presented in Figure 8. The upper section of the SMA bar was rigidly fixed to the second floor. Thus, the stiffness and damping capacity of the TMD were provided by the bending of the SMA. To model the wind action, the ground motion presented in Figure 9 was input using the shaking table. The measurement of acceleration was conducted by accelerometers at a sampling rate of 100 Hz. The testing programme is revealed in Table 1.

Table 1 Testing programme of off-tune

Test number	Mass added on the top floor	With or without TMD	Length of measurement (seconds)	Ground motion input
1	10kg	Without TMD	30	Wind excitation
2		With TMD	30	Wind excitation
3	25kg	Without TMD	30	Wind excitation
4		With TMD	30	Wind excitation
5	30kg	Without TMD	30	Wind excitation
6		With TMD	30	Wind excitation
7	35kg	Without TMD	30	Wind excitation
8		With TMD	30	Wind excitation
9	45kg	Without TMD	30	Wind excitation
10		With TMD	30	Wind excitation

4.2 Results and discussion

Figure 10 shows the acceleration experienced at the top floor measured from Test Nos. 1-10, and a comparison of the structural responses of the conditions with and without the TMD. It can be observed that the structural response under wind excitation can be reduced by installing the TMD when the added mass is 25, 30 and 35 kg. However, the structural response actually increased with 10 and 45 kg added mass after installation of the TMD. According to Figures 10 (a) and (e), the off-tuning of the TMD induces a greater structural response.

The root mean square (RMS) acceleration for each test is shown in Table 2. The reduction percentage in Table 2 indicates the proportion of the structural response reduced by installing the TMD. When the added mass is 30 kg, the RMS acceleration is the smallest, and the reduction percentage is 30.89%, which indicates that the TMD is approaching its most effective status. This can be explained with reference to the optimal design of TMDs where, if the added mass is 30 kg, the design of the natural frequency of the TMD is near optimal, according to Warburton (1982)'s design theory. In that condition, the TMD is capable of vibrating out of phase with the main structure, thus more energy can be dissipated. However, analysis of the off-tuned conditions reveals that the RMS acceleration becomes larger.

Table 2 RMS acceleration [gal] (Test #)

Added mass on top floor (kg)	10	25	30	35	45
With damper	53.0 (2)	33.0 (4)	27.3 (6)	27.4 (8)	30.6 (10)
Without damper	47.7 (1)	46.4 (3)	39.5 (5)	31.4 (7)	28.2 (9)
Reduction percentage	-11.11%	28.88%	30.89%	12.74%	-8.51%

5. Retuning the TMD by changing the SMA temperature under wind excitations

Analysis of the scenarios with an off-tuned TMD demonstrated in Section 4 reveal that, by increasing the added mass from 30 kg to 45 kg, the RMS acceleration was increased by 12.09%. The RMS acceleration rose 20.88% when the added mass decreased from 30 kg to 25 kg. It is important to apply temperature control of the SMA for retuning purposes, with the aim of reducing the structural response after adjusting the natural frequency. The control strategy is shown in Figure 11. To adjust the properties of SMA using temperature control, the cooling process is performed by spraying Tetrafluoroethane while heating is achieved by wrapping the SMA in energised carbon fibre. Experimental testing using these methods shows that SMA can be cooled to −20°C in 1-2 seconds and heated to 45°C in a short period (due to the high thermal conductivity of copper).

5.1 Retuning methods

According to Warburton (1982)'s design theory, when the structural added mass is increased to 45 kg from 30 kg, the expected natural frequency of the TMD becomes 1.46 Hz, as opposed to 1.66 Hz with 30 kg. In order to retune the main structure, the stiffness of the TMD should be decreased by cooling to -25 or -40°C. By implementing this strategy, the natural frequency of the TMD can be adjusted to achieve a result that is approximate to the theoretical expected value. When the added mass decreases to 25 kg from 30 kg, the expected natural frequency of the TMD is 1.71 Hz. The TMD therefore requires heating to 45°C or 65°C so as to increase the natural frequency of the TMD to approach the expected value. The cooling process is conducted by spraying Tetrafluoroethane, whereas heating is implemented by wrapping the SMA in energised carbon fibre. The testing programme is detailed in Table 3.

Table 3 Testing programme of retuning

Test number	Mass added on the top floor	With or without TMD	Length of measurement (seconds)	Ground motion input
11	Increase mass to 45kg	Decrease temperature to -20°C	30	Wind excitation
12		Decrease temperature to -40°C	30	Wind excitation
13	Decrease mass to 25kg	Increase temperature to 45°C	30	Wind excitation
14		Increase temperature to 65°C	30	Wind excitation

5.2 Results: Retuning the TMD when the structural mass increases to 45 kg

Figure 12 compares the acceleration time history at the top floor at room temperature conditions and under cooling. Figures 12 (a) and (b) demonstrate that it is feasible to effectively attenuate the excessive structural response caused by off-tuning by cooling the SMA. It should be noted that the structural response at -40°C is relatively small compared with the response at -20°C. With respect to Table 4, the RMS acceleration of 20.0 gal in Test 12 is significantly smaller than the corresponding result in Test 10 of 30.6 gal. Furthermore, 34.64% of the RMS acceleration was reduced through cooling the SMA to -40°C from 19°C.

There are two reasons behind the effective reduction in structural response by cooling. First, the natural frequency of the TMD was retuned to the expected frequency range. Secondly, the damping ratio can be increased by cooling and, in particular, rises significantly from -20°C to -40°C. As the damping ratio of the SMA-based TMD included in this study was not optimally designed and lower than the expected value, the increased damping ratio by cooling to -40°C can partially compensate for this deficiency and, therefore, facilitate the structural response reduction.

Table 4 The structural response with added mass of 45kg after re-tuning the TMD by cooling the SMA

Temperature of damper (°C)	Test number	RMS acceleration (gal)	Reduction Percentage
-40	12	20.0	34.64%
-20	11	21.4	30.07%
19	10	30.6	reference

5.3 Results: Retuning the TMD when the structural mass decreases to 25 kg

Figures 13 (a) and (b) present the structural response experienced when the SMA-based TMD was heated to 45°C and 65°C (Test 13 and 14), respectively. It can be observed that the structural response was not reduced via heating. According to Table 5, the RMS acceleration was increased by

3.94% when the heating process was conducted on the SMA. The results demonstrate that the effectiveness of heating the SMA to retune the TMD is non-significant. This could be due to the stiffness of the SMA at a temperature greater than 19℃ being insensitive to temperature, which in turn provides a smaller variance. Moreover, heating causes a loss of damping, which degrades the energy dissipation capacity of the TMD.

Table 5 The structural response with added mass of 25kg after re-tuning the TMD by heating the SMA

Temperature of damper (℃)	Test number	RMS acceleration (gal)	Reduction Percentage
65	14	34.3	-3.94%
45	13	34.2	-3.64%
19	4	33.0	reference

5.4 Discussion

The phase transformation temperature range of the SMA applied during this study is from -25℃ to 5℃. The variance of the mechanical properties is large when the SMA is cooled to -20 and -40℃ from 19℃, because the SMA transforms to martensite from austenite. If the phase transformation temperature range of the SMA can be adjusted to the higher temperature, the effectiveness of the SMA-based TMD for temperature control at a higher temperature than 19℃, can be improved. In future studies, SMAs with higher phase transformation temperatures should be investigated in terms of their application in semi-active TMDs.

In applications designed to resist wind-induced vibration, the fatigue life of the SMA is particularly important. Therefore, it is essential to study the characteristics of the Cu-Al-Mn SMA under small strain level deformation. As indicated in our previous material studies, which analysed a SMA bar under dynamic bending, the secant stiffness and equivalent viscous damping ratio tend to be smaller in the first 100 cycles in both Cu-Al-Mn and Ni-Ti SMAs. Similar instability of SMAs in the initial cycles has been previously studied (Eggeler et al., 2004, Soul et al., 2010, Khan et al., 2013). The cause of this instability has been attributed to the dislocation slip between grains, where the internal stress caused by the slip influences the dynamic properties. In order to overcome this problem, Hartl et al. (2010) conducted 100 thermal cycles with a constant stress on the SMA and found the transformation strain become insensitive to the loading cycles. According to previous studies (Shaw and Kyriakides, 1995, Khan et al., 2013, Miyazaki et al., 1986), appropriate annealing treatment can generate stable behaviours in the SMA. Moreover, cyclic loading as a form of 'pre-training' is also an effective method to stabilise the dynamic properties of the SMA. Thus, in future investigations on SMA-based TMDs, the stabilisation of the SMA should be considered.

When applied to real civil structures, the SMA-based TMD should be of a larger size and thus the efficiency of the temperature control needs to be considered. Copper has a better thermal conductivity than that of other elements comprising SMA, e.g. nickel and titanium, which means that copper-based SMA such Cu-Al-Mn SMA is preferred in real applications. The SMA-based TMD can also employ multiple SMA bars in parallel. Heating and cooling multiple SMA bars can speed up the temperature control and increase its accuracy. This is because, in this combined system, separate bars can be heated and cooled concurrently, enabling the control of both the natural frequency and the damping ratio at a near optimal level of design. The application of multiple SMA bars can be effective in providing an adequate damping ratio in the event of damping loss when heating. The use of multiple SMA bars as a control strategy will be investigated in further studies.

In a future extension of this study, one single SMA-based TMD can be replaced by SMA-based multi-TMD (MTMD) system. MTMD means that more than one TMD is installed on the structure in parallel or in series (Nigdeli and Bekdas, 2019, Arfiadi, 2016). MTMD can distribute natural frequency and can be designed to tune several modes of structural vibration. Consequently, the vibration amplitude can be reduced further in a wider frequency range.

The optimal TMD design method used in this study is the Warburton method (Warburton, 1982), because this study was conducted on a laboratory scale. More precise and effective optimal design methods are required by the full-scale SMA-based tuned mass damper to control large-size structures. Bekdaş and Nigdeli (2011), Nigdeli and Bekdas (2013), Bekdaş et al. (2017), and Nigdeli and Bekdaş (2017) have developed optimal design methods employing the harmony search algorithm. Optimal design methods employing novel algorithms such as Particle swarm optimisation algorithm (Leung and Zhang, 2009) and machine learning algorithm (Yucel et al., 2019) have recently developed and can be incorporated into the SMA-based TMD to increase the tuning efficiency in future research. Structures not only sustain wind loads; they also suffer seismic loads. Therefore, a reduction in seismic vibration should be taken into consideration in the optimal design procedures employed in further studies of SMA-based TMD (Pourzeynali et al., 2013, Farshidianfar and Soheilia, 2013, Nigdeli and Bekdas, 2014, Bekdaş et al., 2018, Bekdaş et al., 2019).

Wind can cause simultaneous horizontal loadings and vertical loadings on the structure. For tall structures and flexible structures, the vertical stiffness is much larger in comparison to the horizontal stiffness and thus the vertical loads exert only a minimal effect on the vertical axis force on the structure. In such cases, the wind loadings in the calculation can be assumed to be horizontal actions. However, the vertical loads of wind greatly affect the vibration of space structures and long-span structures, and thus should be taken into consideration in the design process. In the tested steel framed structure used in this study, the column-beam connections were built as hinge joints with three parallel springs to facilitate rotation. The steel framed structure was therefore flexible in the horizontal direction. Thus, the wind loads were simplified as horizontal actions. Furthermore, due to the single-degree-of-freedom limitation of the shaking table in the laboratory, the wind loads can only be excited horizontally. For civil engineering applications, both horizontal and vertical wind loadings should be considered in the analytical model to ensure an accurate design.

6. Conclusion

In this study, SMA was applied to retune an off-tuned TMD to reduce wind-induced vibration. By material characterisation of Cu-Al-Mn SMA, the stiffness increases and damping ratio decreases with rising temperature. The stiffness and damping ratio are sensitive to temperature when the in-service temperature is near the phase transformation temperature range.

The wind excitation in this study was generated through application of the AR method and was imposed by ground motion using a shaking table. The results demonstrate that the wind-induced vibration of the steel framed structure can be attenuated effectively by installing a SMA-based TMD. However, by increasing and decreasing the main structural mass to instigate off-tuning, the structural response became larger. The RMS acceleration shows an increase of up to 20.88% when the TMD is off-tuned. The effectiveness of cooling SMA is significant in terms of retuning the off-tuned TMD, because the stiffness variance is large between -25℃ and 5℃ and the damping was increased. However, heating the SMA presents limited effectiveness in retuning the TMD, since the stiffness of the SMA is insensitive at temperatures greater than 19℃ and damping is reduced. In further studies, SMAs with higher phase transformation temperatures will be applied, and the control theory for multiple SMA bars as well other approaches will be investigated in order to increase the damping capacity of the TMD.

Acknowledgement

The authors would like to thank funding from National Natural Science Foundation of China (51908007), Beijing Municipal Education Commission (KM201910005021) and International Copper Association for financial support (TEK-1079), and also thank Shinko Metal Product Co., LTD for their shape memory alloy supply.

References:

AGUIAR, R. A. A., SAVI, M. A. & PACHECO, P. M. C. L. 2013. Experimental investigation of vibration reduction using shape memory alloys. Journal of Intelligent Material Systems and Structures, 24, 247-261.

ANDRAWES, B. & DESROCHES, R. 2007. Effect of ambient temperature on the hinge opening in bridges with shape memory alloy seismic restrainers. Engineering structures, 29, 2294 - 2301.

ARAYA, R., MARIVIL, M., MIR, C., MORONI, O. & SEPULVEDA, A. 2008. Temperature and grain size effects on the behavior of CuAlBe SMA wires under cyclic loading. Materials science and engineering A - structural materials properties microstructure and processing, 496, 209-213.

ARFIADI, Y. 2016. Reducing Response of Structures by Using Optimum Composite Tuned Mass Dampers. Procedia Engineering, 161, 67-72.

BEKDAŞ, G., KAYABEKIR, A. E., NIGDELI, S. M. & TOKLU, Y. C. 2019. Tranfer function amplitude minimization for structures with tuned mass dampers considering soil-structure interaction. Soil Dynamics and Earthquake Engineering, 116, 552-562.

BEKDAŞ, G. & NIGDELI, S. M. 2011. Estimating optimum parameters of tuned mass dampers using harmony search. Engineering Structures, 33, 2716-2723.

BEKDAŞ, G., NIGDELI, S. M. & YANG, X.-S. 2017. Metaheuristic Based Optimization for Tuned Mass Dampers Using Frequency Domain Responses. In: DEL SER, J., ed. Harmony Search Algorithm, 2017// 2017 Singapore. Springer Singapore, 271-279.

BEKDAŞ, G., NIGDELI, S. M. & YANG, X.-S. 2018. A novel bat algorithm based optimum tuning of mass dampers for improving the seismic safety of structures. Engineering Structures, 159, 89-98.

BRINCKER, R., RODRIGUES, J. & ANDERSEN, P. 2004. Scaling the mode shapes of a building model by mass changes. IMAC-22: A Conference on Structural Dynamics. Hyatt Regency Dearborn, Dearborn, Michigan, USA: Society for Experimental Mechanics.

CHANG, W.-S. & ARAKI, Y. 2016. Use of shape-memory alloys in construction: a critical review. Proceedings of the Institution of Civil Engineers - Civil Engineering, 169.

CONNOR, J. & LAFLAMME, S. 2014. Structural motion engineering, New York, Springer.

DAVENPORT, A. G. 1961. The spectrum of horizontal gustiness near the ground in high winds. Quarterly Journal of the Royal Meteorological Society, 87, 194-211.

DEN HARTOG, J. P. 1956. Mechanical vibrations, New York ; London, McGraw-Hill.

EGGELER, G., HORNBOGEN, E., YAWNY, A., HECKMANN, A. & WAGNER, M. 2004. Structural and functional fatigue of NiTi shape memory alloys. Materials Science and Engineering a-Structural Materials Properties Microstructure and Processing, 378, 24-33.

ELAHINIA, M. H., KOO, J. H. & TAN, H. 2005. Improving robustness of tuned vibration absorbers using shape memory alloys. Shock and Vibration, 12, 349-361.

FARSHIDIANFAR, A. & SOHEILIA, S. 2013. ABC optimization of TMD parameters for tall buildings with soil structure interaction. Interaction and Multiscale Mechanics, 6, 339-365.

FISCO, N. R. & ADELI, H. 2011. Smart structures: Part I-Active and semi-active control. Scientia Iranica, 18, 275-284.

HADI, M. N. S. & ARFIADI, Y. 1998. Optimum design of absorber for MDOF structures. JOURNAL OF STRUCTURAL ENGINEERING-ASCE, 124, 1272-1280.

HARTL, D. J., LAGOUDAS, D. C., CALKINS, F. T. & MABE, J. H. 2010. Use of a Ni60Ti shape memory alloy for active jet engine chevron application: I. Thermomechanical characterization. Smart Materials & Structures, 19.

HUANG, H. & CHANG, W.-S. 2018. Application of pre-stressed SMA-based tuned mass damper to a timber floor system. Engineering Structures 167, 143-150.

HUANG, H., MOSALAM, K. M. & CHANG, W.-S. 2020a. Temperature-controlled adaptive tuned mass damper with shape memory alloy for seismic application. Earthquake Engineering and Structral Dynamics, (Under Review).

HUANG, H., ZHU, Y.-Z. & CHANG, W.-S. 2020b. Comparison of Bending Fatigue of NiTi and CuAlMn Shape Memory Alloy Bars. Advances in Materials Science and Engineering, 2020, 1-9.

HUANG, H. Y., CHANG, W. S. & MOSALAM, K. M. 2017. Feasibility of shape memory alloy in a tuneable mass damper to reduce excessive in-service vibration. Structural Control & Health Monitoring, 24, 1-14.

INDIRLI, M., FORNI, M. & MARTELLI, A. 2001. Further new projects in Italy for the development of innovative techniques for the seismic protection of cultural heritage. Proceedings of the 7th International Seminar on Seismic Isolation, Passive Energy Dissipation and Active Control of Vibrations of Structures, 2001 Assisi, Italy.

IRWIN, P., KILPATRICK, J., ROBINSON, J. & FRISQUE, A. 2008. Wind and Tall Buildings: Negatives and Positives. Structural Design of Tall and Special Buildings, 17, 915-928.

ISLAM, M. S., DO, J. & KIM, D. 2018. Multi-Objective Optimization of TMD for Frame Structure Based on Response Surface Methodology and Weighted Desirability Function. KSCE Journal of Civil Engineering, 22, 3015-3027.

JIANG, G. L. & HANAGAN, L. M. 2006. Semi-active TMD with piezoelectric friction dampers in floor vibration control - art. no. 616915. Smart Structures and Materials 2006: Damping and Isolation, 6169, 16915-16915.

KANG, J., KIM, H. S. & LEE, D. G. 2011. Mitigation of wind response of a tall building using semi-active tuned mass dampers. Structural Design of Tall and Special Buildings, 20, 552-565.

KHAN, M. I., KIM, H. Y., NAMIGATA, Y., NAM, T. H. & MIYAZAKI, S. 2013. Combined effects of work hardening and precipitation strengthening on the cyclic stability of TiNiPdCu-based high-temperature shape memory alloys. Acta Materialia, 61, 4797-4810.

LEUNG, A. Y. T. & ZHANG, H. 2009. Particle swarm optimization of tuned mass dampers. Engineering Structures, 31, 715-728.

LIANG, D. & LIU, T. 2012. Time history analysis of the impact of the vertical wind vibration to the light weight steel factory buildings of portal frames. Journal of Civil Engineering and Construction, 1, 32-37.

MANI, Y. & SENTHILKUMAR, M. 2015. Shape memory alloy-based adaptive-passive dynamic vibration absorber for vibration control in piping applications. Journal of Vibration and Control, 21, 1838-1847.

MIGUEL, L. F. F., LOPEZ, R. H., TORII, A. J., MIGUEL, L. F. F. & BECK, A. T. 2016. Robust design optimization of TMDs in vehicle–bridge coupled vibration problems. Engineering Structures, 126, 703-711.

MIYAZAKI, S., IMAI, T., IGO, Y. & OTSUKA, K. 1986. Effect of cyclic deformation on the pseudoelasticity characteristics of Ti-Ni alloys. Metallurgical Transactions a-Physical Metallurgy and Materials Science, 17, 115-120.

NAGARAJAIAH, S. & SONMEZ, E. 2007. Structures with semiactive variable stiffness single/multiple tuned mass dampers. Journal of structural engineering-Asce, 133, 67-77.

NAGARAJAIAH, S. & VARADARAJAN, N. 2005. Short time Fourier transform algorithm for wind response control of buildings with variable stiffness TMD. Engineering Structures, 27, 431-441.

NIGDELI, S. M. & BEKDAS, G. 2013. Optimum tuned mass damper design for preventing brittle fracture of RC buildings. Smart Structures and Systems, 12, 137-155.

NIGDELI, S. M. & BEKDAS, G. 2014. Optimum tuned mass damper approaches for adjacent structures. Earthquakes and Structures, 7, 1071-1091.

NIGDELI, S. M. & BEKDAS, G. 2019. Optimum design of multiple positioned tuned mass dampers for structures constrained with axial force capacity. Structural Design and Special Buildings, 28, e1593.

NIGDELI, S. M. & BEKDAŞ, G. 2017. Optimum tuned mass damper design in frequency domain for structures. KSCE Journal of Civil Engineering, 21, 912-922.

POURZEYNALI, S., SALIMI, S. & EIMANI KALESAR, H. 2013. Robust multi-objective optimization design of TMD control device to reduce tall building responses against earthquake excitations using genetic algorithms. Scientia Iranica, 20, 207-221.

RUSTIGHI, E., BRENNAN, M. J. & MACE, B. R. 2005. A shape memory alloy adaptive tuned vibration absorber: design and implementation. Smart materials & structures, 14, 19-28.

SADEK, F., MOHRAZ, B., TAYLOR, A. W. & CHUNG, R. M. 1997. A method of estimating the parameters of tuned mass dampers for seismic applications. Earthquake Engineering & Structural Dynamics, 26, 617-635.

SARKAR, T. K. & PEREIRA, O. 1995. Using the Matrix Pencil Method to Estimate the Parameters of a Sum of Complex Exponentials. Ieee Antennas and Propagation Magazine, 37, 48-55.

SAVI, M. A., DE PAULA, A. S. & LAGOUDAS, D. C. 2011. Numerical Investigation of an Adaptive Vibration Absorber Using Shape Memory Alloys. Journal of Intelligent Material Systems and Structures, 22, 67-80.

SHAW, J. A. & KYRIAKIDES, S. 1995. Thermomechanical aspects of NiTi. Journal of the mechanics and physics of solids, 43, 1243-1281.

SOROUSHIAN, P., OSTOWARI, K., NOSSONI, A. & CHOWDHURY, H. 2001. Repair and strengthening of concrete structures through application of corrective posttensioning forces with shape memory alloys. Design of Structures 2001, 20-26.

SOUL, H., ISALGUE, A., YAWNY, A., TORRA, V. & LOVEY, F. C. 2010. Pseudoelastic fatigue of NiTi wires: frequency and size effects on damping capacity. Smart Materials & Structures, 19.

SUN, W.-Q. & LI, Q.-B. 2009. TMD semi-active control with shape memory alloy. Journal of Harbin Institute of Technology, 41, 164-168.

TISEO, B., CONCILIO, A., AMEDURI, S. & GIANVITO, A. 2010. A Shape Memory Alloys Based Tuneable Dynamic Vibration Absorber for Vibration Tonal Control. Journal of Theoretical and Applied Mechanics, 48, 135-153.

TORRA, V., ISALGUE, A., AUGUET, C., CARRERAS, G., LOVEY, F. C., SOUL, H. & TERRIAULT, P. 2009. Damping in civil engineering using SMA. The fatigue behavior and stability of CuAlBe and NiTi alloys. Journal of Materials Engineering and Performance, 18, 738-745.

TSAI, H. C. & LIN, G. C. 1993. Optimum Tuned-Mass Dampers for Minimizing Steady-State Response of Support-Excited and Damped Systems. Earthquake Engineering & Structural Dynamics, 22, 957-973.

WARBURTON, G. B. 1982. Optimum Absorber Parameters for Various Combinations of Response and Excitation Parameters. Earthquake Engineering & Structural Dynamics, 10, 381-401.

WILLIAMS, K., CHIU, G. & BERNHARD, R. 2002. Adaptive-passive absorbers using shape-memory alloys. Journal of sound and vibration, 249, 835-848.

WILLIAMS, K. A., CHIU, G. T. C. & BERNHARD, R. J. 2005. Dynamic modelling of a shape memory alloy adaptive tuned vibration absorber. Journal of Sound and Vibration, 280, 211-234.

XUE, S., TANG, H., OKADA, J., HAYASHI, T., ZONG, G. & ARIKAWA, S. 2009. Natural frequency changes for damaged and reinforced real structure in comparison with shake table and simulation. Materials forum, 33, 344-350.

YANG, J. N., AGRAWAL, A. K., SAMALI, B. & WU, J. C. 2001. A benchmark problem for response control of wind-excited tall buildings. Proceedings of Imac-Xix: A Conference on Structural Dynamics, Vols 1 and 2, 4359, 151-157.

YUCEL, M., BEKDAŞ, G., NIGDELI, S. M. & SEVGEN, S. 2019. Estimation of optimum tuned mass damper parameters via machine learning. Journal of Building Engineering, 26, 100847.

ZIELIŃSKI, T. P. & DUDA, K. 2011. Frequency and damping estimation methods - an overview. Metrology and measurement systems, 18, 505 - 528.

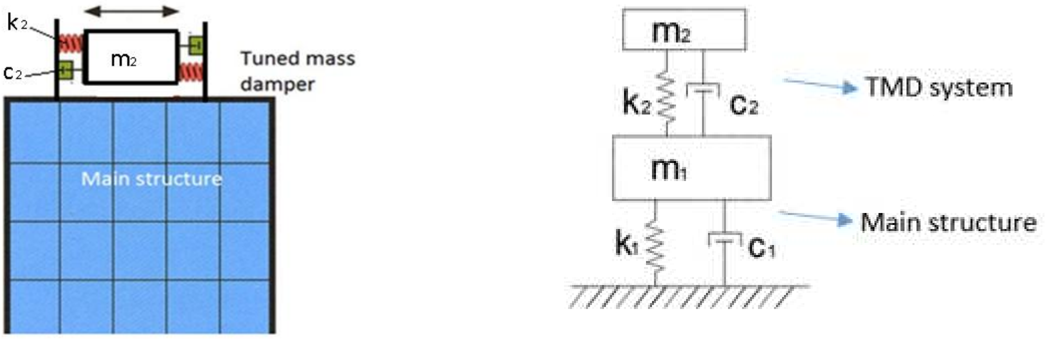

(a) (b)

Figure 1 (a) Simulation of the TMD installed on a structure; (b) Idealisation of TMD model

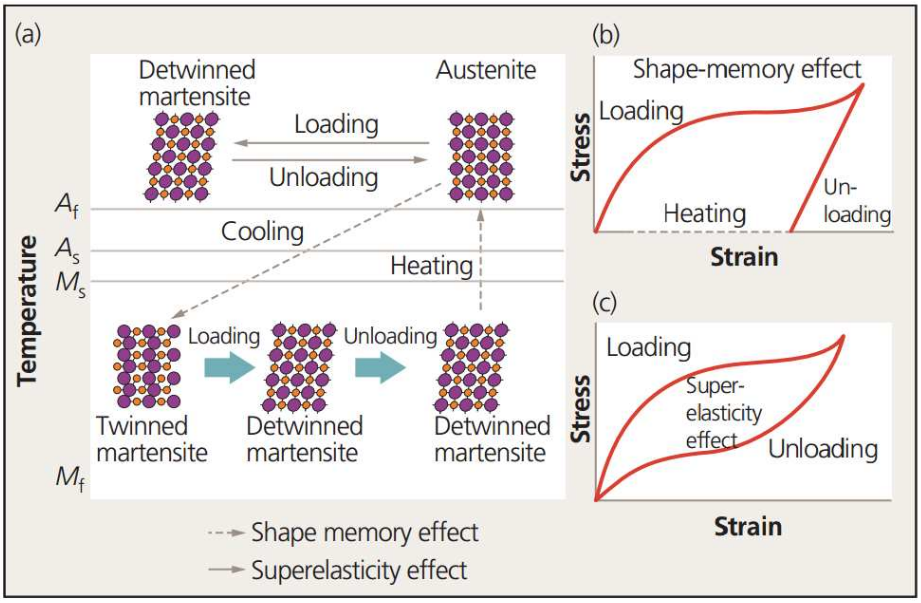

Figure 2 (a) Different phases of shape-memory alloy at different temperatures and stress-strain curve demonstrating the (b) shape memory effect; (c) superelasticity (cited by (Chang and Araki, 2016))

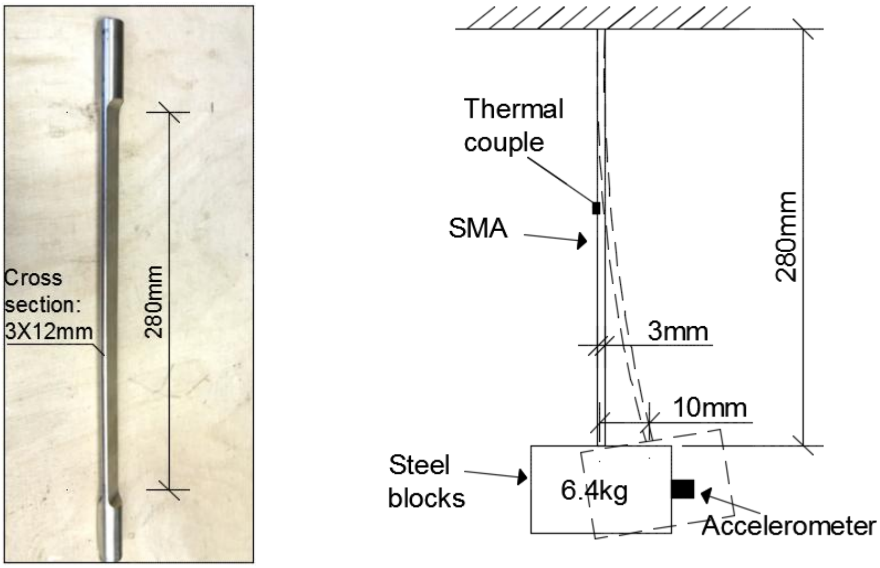

(a) (b)

Figure 3 (a) Cu-Al-Mn SMA bar applied in the test;(b) Set-up of single SMA-based damper free vibration tests (drawing not to scale) (cited by Huang et al. (2020a))

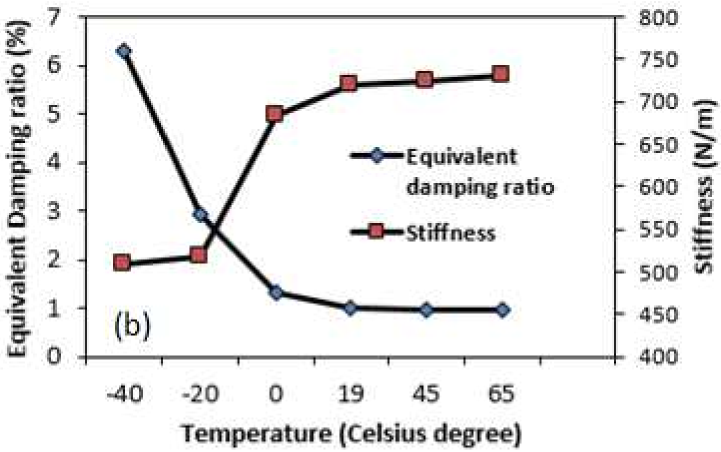

Figure 4 Effect of temperature on stiffness and damping ratio (cited by Huang et al. (2020a))

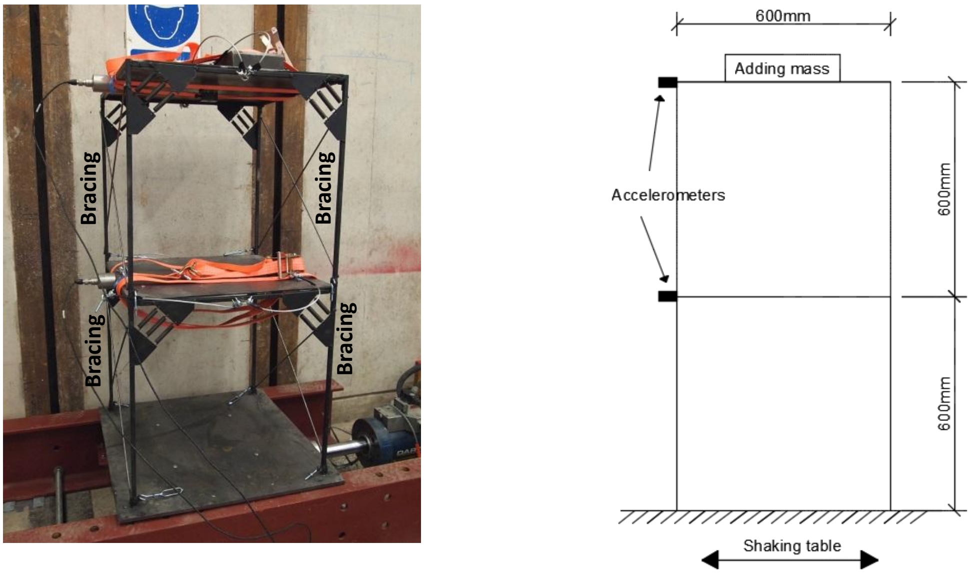

(a) (b)

Figure 5 (a) Steel frame applied to this study as the main structure; (b) Dimensions of the steel frame (cited by Huang et al. (2020a))

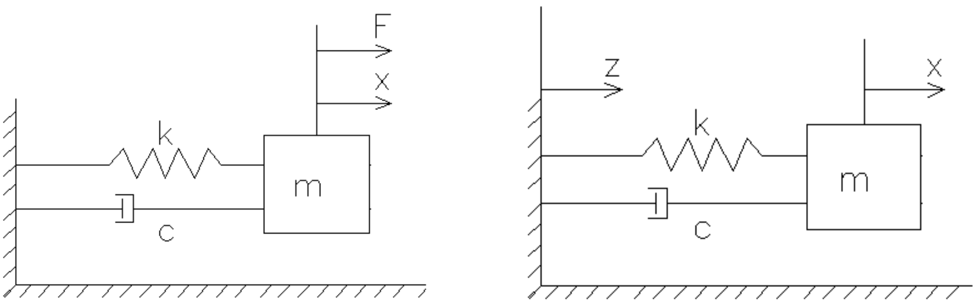

(a) (b)

Figure 6 (a) Forced vibration system; (b) Base-excited system

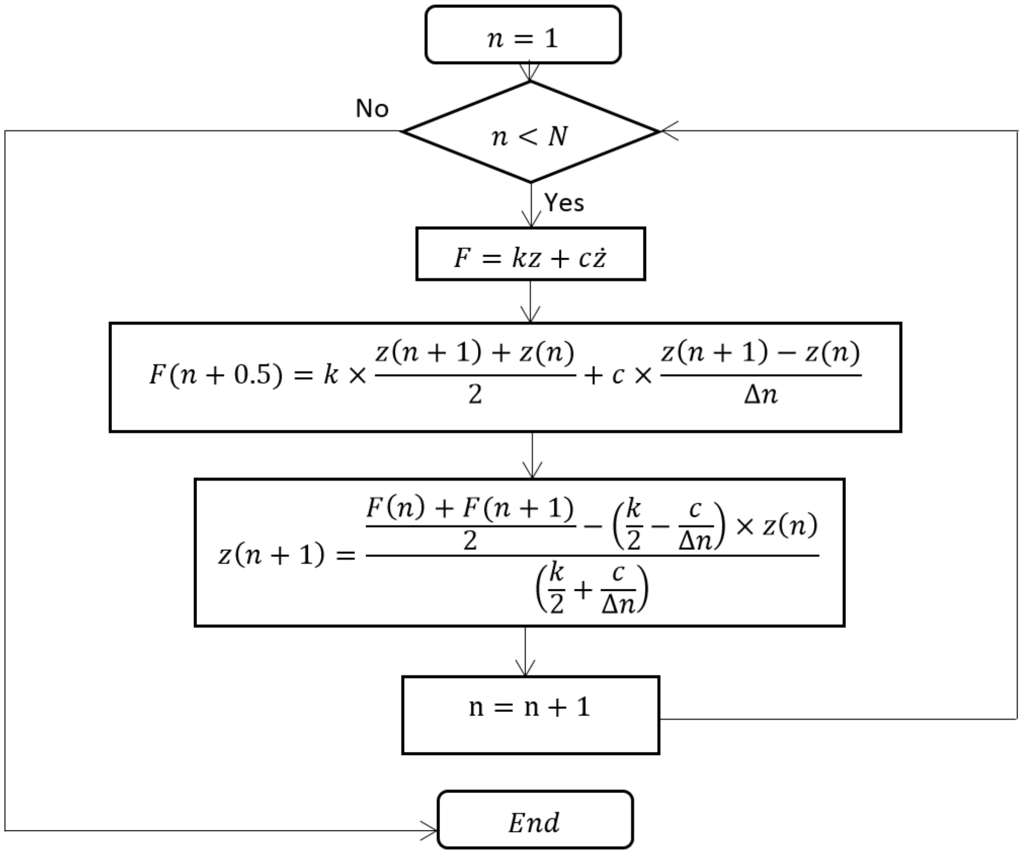

Figure 7 Flow diagram for calculating ground motion to model wind action

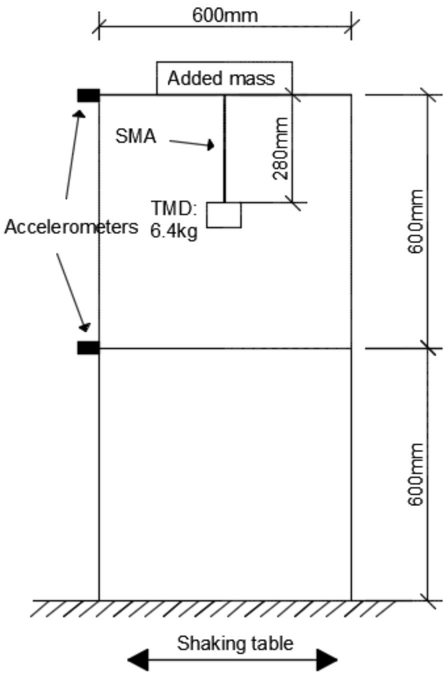

Figure 8 Installation of the SMA-based TMD on the steel frame and shaking table tests set-up (cited by Huang et al. (2020a))

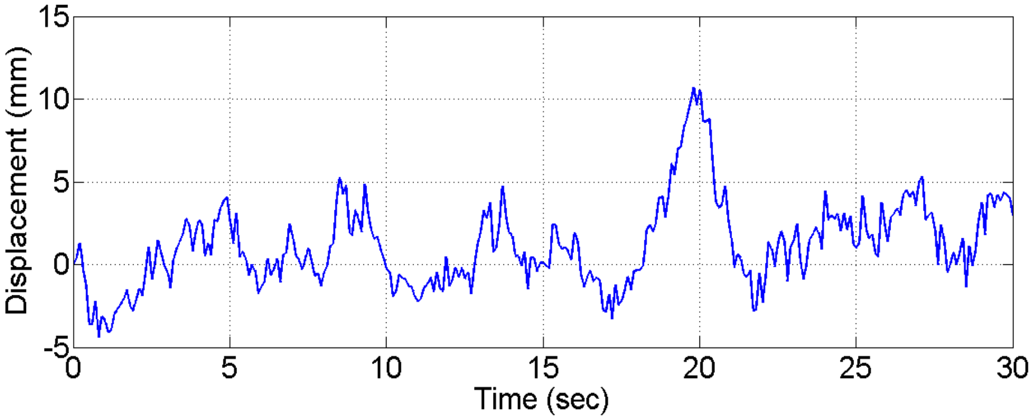

Figure 9 Ground motion modelling the wind action

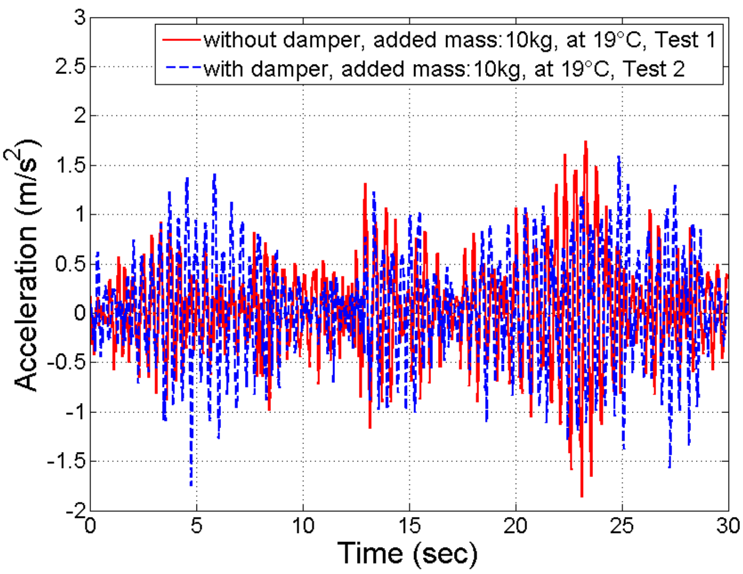

(a)

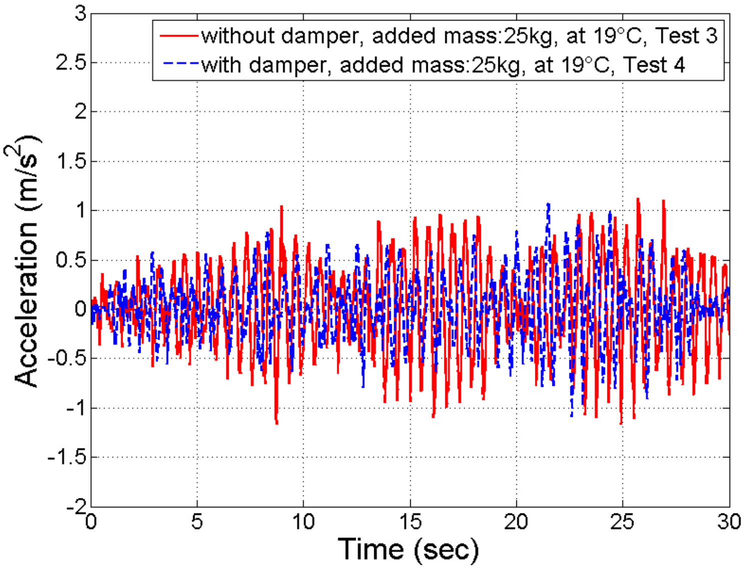
without damper, added mass:25kg, at 19°C, Test 3
with damper, added mass:25kg, at 19°C, Test 4
Acceleration (m/s²)
Time (sec)
3
2.5
2
1.5
1
0.5
0
-0.5
-1
-1.5
-2
0
5
10
15
20
25
30

(b)

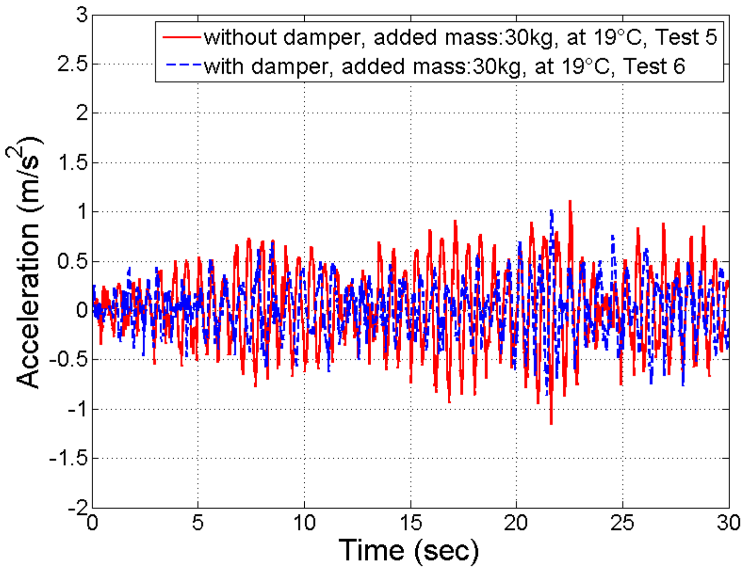
without damper, added mass:30kg, at 19°C, Test 5
with damper, added mass:30kg, at 19°C, Test 6
Acceleration (m/s²)
Time (sec)
3
2.5
2
1.5
1
0.5
0
-0.5
-1
-1.5
-2
0
5
10
15
20
25
30

(c)

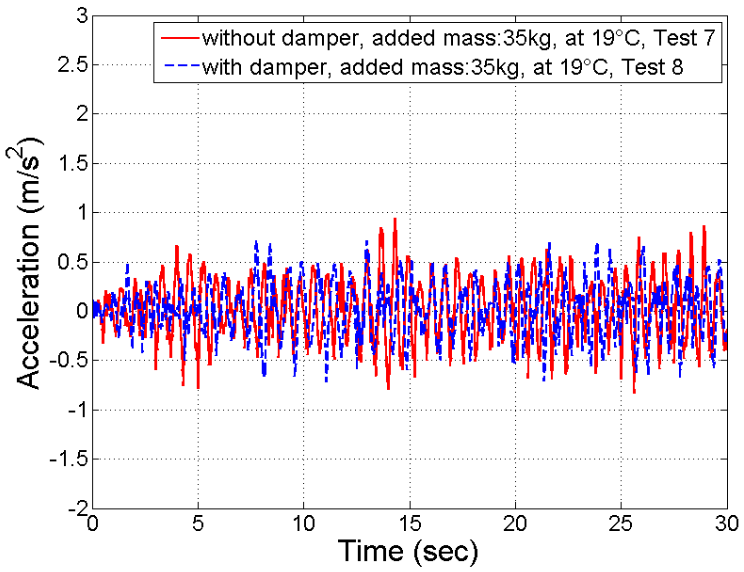

(d)

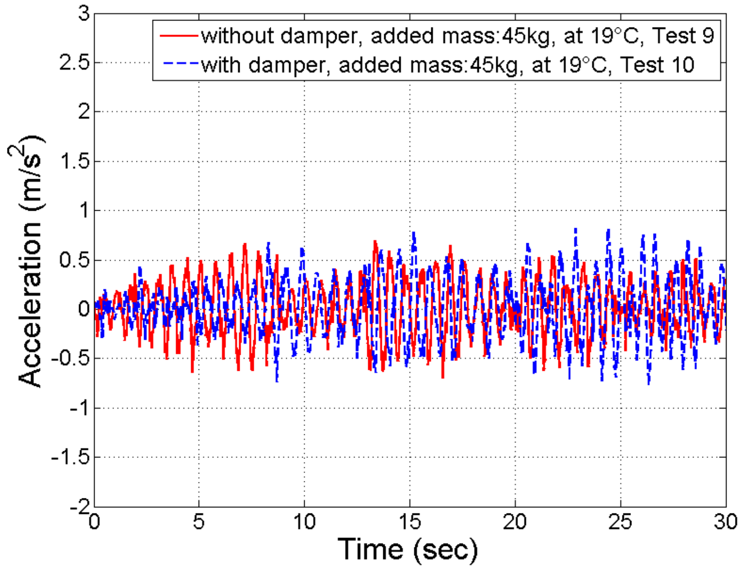

(e)

Figure 10 Structural response with and without TMD under wind excitation when added mass is (a) 10kg; (b) 25kg; (c) 30kg; (d) 35kg and (e) 45kg

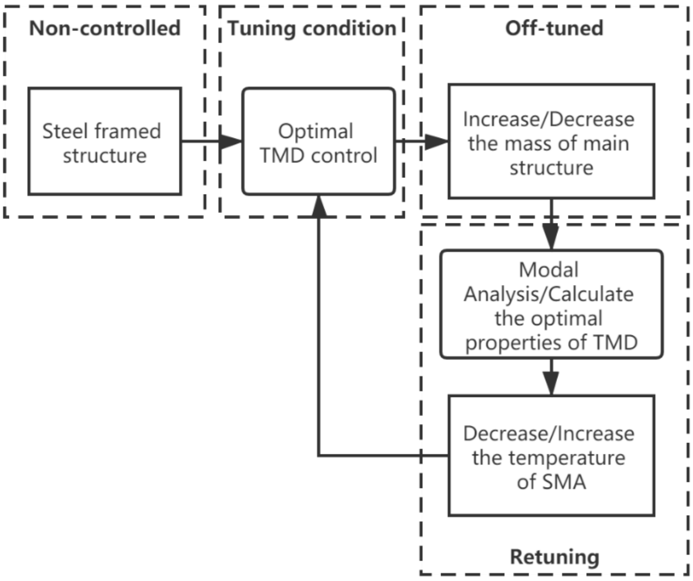

Figure 11 Control strategy of the SMA-based TMD

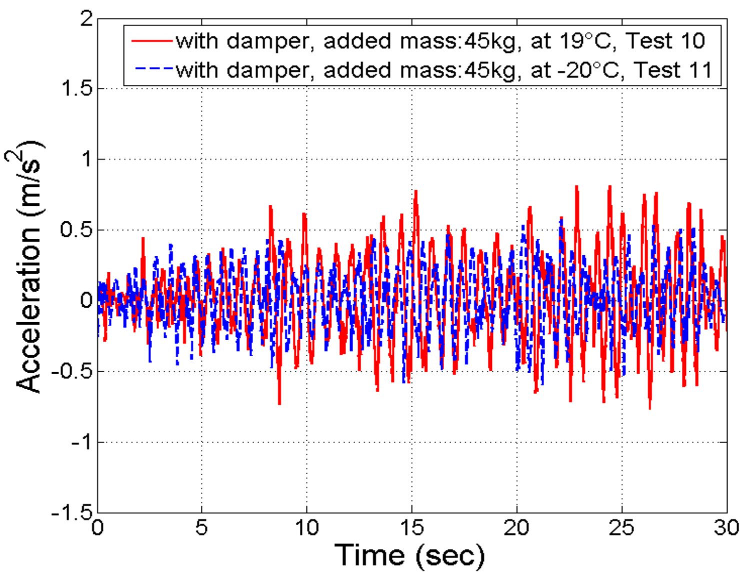

(a)

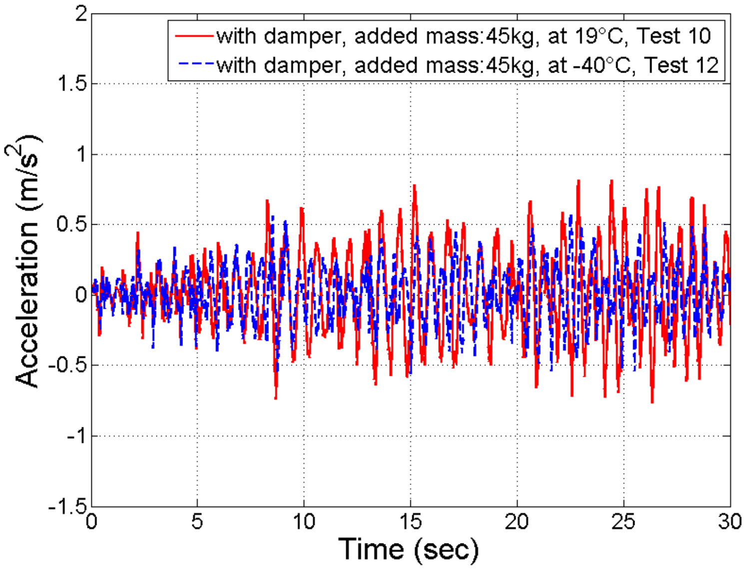

(b)

Figure 12 Comparison of the structural response with TMD under the wind excitation (a) at between 19℃ and -20℃; (b) at between 19℃ and -40℃

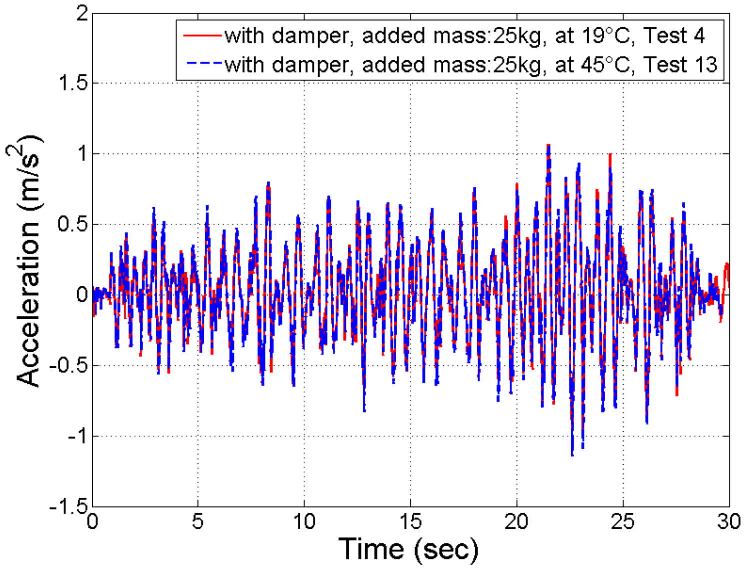

(a)

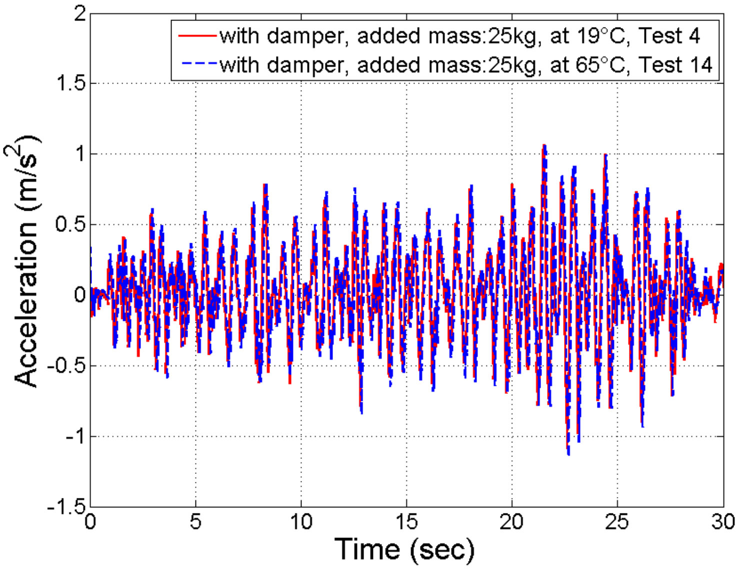

(b)

Figure 13 Comparison of the structural response with TMD under the wind excitation (a) between 19℃ and 45℃; (b) between 19℃ and 65℃

Figure captions

Figure 1 (a) Simulation of the TMD installed on a structure; (b) Idealisation of TMD model

Figure 2 (a) Different phases of shape-memory alloy at different temperatures and stress-strain curve demonstrating the (b) shape memory effect; (c) superelasticity (cited by (Chang and Araki, 2016))

Figure 3 (a) Cu-Al-Mn SMA bar applied in the test;(b) Set-up of single SMA-based damper free vibration tests (drawing not to scale) (cited by Huang et al. (2020a))

Figure 4 Effect of temperature on stiffness and damping ratio (cited by Huang et al. (2020a))

Figure 5 (a) Steel frame applied to this study as the main structure; (b) Dimensions of the steel frame (cited by Huang et al. (2020a))

Figure 6 (a) Forced vibration system; (b) Base-excited system

Figure 7 Flow diagram for calculating ground motion to model wind action

Figure 8 Installation of the SMA-based TMD on the steel frame and shaking table tests set-up (cited by Huang et al. (2020a))

Figure 9 Ground motion modelling the wind action

Figure 10 Structural response with and without TMD under wind excitation when added mass is (a) 10kg; (b) 25kg; (c) 30kg; (d) 35kg and (e) 45kg

Figure 11 Control strategy of the SMA-based TMD

Figure 12 Comparison of the structural response with TMD under the wind excitation (a) at between 19°C and -20°C; (b) at between 19°C and -40°C

Figure 13 Comparison of the structural response with TMD under the wind excitation (a) between 19℃ and 45℃; (b) between 19℃ and 65℃

***Detailed Response to Reviewers**

Dear Editor,

Please find tables which we respond to all the comments that reviewers have, we have considered comments from reviewers, responded and amended our manuscript as appropriate. The comments from reviewers are very useful to improve the quality of the manuscript, their efforts and time are much appreciated. We are looking forward to working with you during the review process.

Best regards,

Wen-Shao Chang

Reviewer #4:

Reviewer's comments	Response to reviewer
(1) How to use the SMA in TMD, this information is lacking. For example, How is the SMA arranged in the TMD device in this study? How fast is the shape memory alloy heating and cooling? What is the control strategy? Does these affect control frequency, accuracy, and application of actual semi-active control?	The authors agree with the reviewer's comments. The questions raised are answered in turn below. The non-pre-stressed SMA-based TMD described in Section 2, as shown in Figure 3 (b), was installed on the steel framed structure as shown in Figure 5 vertically. The installation of the SMA-based TMD is presented in Figure 8. The upper section of the SMA bar was rigidly fixed to the second floor. Thus, the stiffness and damping capacity of the TMD were provided by the bending of the SMA. Figure 8 has been added in the manuscript to show the arrangement of the SMA-based TMD. The explanation above has been included in the first paragraph in Section 4.1 and is marked in red. It is important to apply temperature control of the SMA for retuning purposes. The aim is to reduce the structural response after adjusting the natural frequency. The control strategy is shown in Figure 11. To adjust the properties of SMA using temperature control, the cooling process is performed by spraying Tetrafluoroethane while heating is achieved by wrapping the SMA in energised carbon fibre. Experimental testing using these methods shows that SMA can be cooled to -20℃ in 1-2 seconds and heated to 45℃ in a short period (due to the high thermal conductivity of copper). The explanation above has been included in the first paragraph of Section 5 and is marked in red. When applied to real civil structures, the SMA-based TMD should be of a larger size and thus the efficiency of the temperature control needs to be considered. Copper has a better thermal conductivity than that of other elements comprising SMA, e.g. nickel and titanium, which means that copper-based SMA such Cu-Al-Mn SMA is preferred in real applications. The SMA-based TMD can also employ multiple SMA bars in parallel. Heating and cooling multiple SMA bars can speed up the temperature control and increase its accuracy. This is because, in this combined system, separate bars can be heated and cooled concurrently, enabling the control of both the natural frequency and the damping ratio at a near optimal level of design. The application of multiple SMA bars can be effective in providing

	an adequate damping ratio in the event of damping loss when heating. The use of multiple SMA bars as a control strategy will be investigated in further studies. The explanation above has been included in the third paragraph of Section 5.4 and is marked in red.
(2) Please provide a full description of linear-prediction singular-value decomposition-based matrix pencil method in section 2.1. How is it calculated and how do the Numbers justify the results?	The authors agree with the reviewer's comments. The natural frequency and equivalent viscous damping ratio were computed using the linear-prediction singular-value decomposition-based matrix pencil (SVD-MP) method. This approach is able to deal with the approximation for complex exponentials and exhibits high precision in estimating the frequency and damping from measured data. Detailed descriptions can be found in Sarkar and Pereira (1995) and Zieliński and Duda (2011). The SVD-MP approach is based on Equations (2) and (3): $$y(t) = x(t) + n(t) \approx \sum_{i=1}^{M} R_i \exp(s_i t) + n(t); 0 \leq t \leq T \quad (2)$$ where $y(t)$ is the observed time response, $x(t)$ is the signal, $n(t)$ is the noise in system, and R_i denotes the complex amplitudes. s_i is presented in Equation (3): $$s_i = -\alpha_i + j\omega_i \quad (3)$$ where α_i and ω_i represent the damping factors and the angular frequencies, respectively, and $j = \sqrt{-1}$. As shown in Equation (2), the objective of SVD-MP is to estimate the frequencies and damping factors from the noise-contaminated data. Thus, solving the parameters is a non-linear problem. According to the equation derivations in Sarkar and Pereira (1995), the matrix pencil is a one-step process for solving a non-linear problem that is computationally efficient. Linear-prediction singular-value decomposition provides a method for decomposing the eigenvectors when using the matrix pencil. The explanation above has been included in the second paragraph of Section 2.1 and is marked in red.
(3) In general, it takes some time to change the elastic modulus of SMA or to generate the driving force, and the material itself has	The authors agree with the reviewer's comments. The material characterisation of Cu-Al-Mn SMA bars under dynamic bending was performed in our

hysteresis. In this respect, what are the properties of the shape memory alloys used in this study?	previous material study (Huang et al., 2020). The material hysteresis, stiffness, damping ratio, and fatigue life were studied under strain levels of 0.5%, 1%, 2%, and 6%. The test results showed Cu-Al-Mn SMA has stable material properties along the dynamic loading and an adequate fatigue life. The explanation above has been included in the first paragraph of Section 2.1 and is marked in red. For the properties of Cu-Al-Mn SMA, please refer to our paper : HUANG, H., ZHU, Y.-Z. & CHANG, W.-S. 2020. Comparison of Bending Fatigue of NiTi and CuAlMn Shape Memory Alloy Bars. Advances in Materials Science and Engineering, 2020, 1-9.
(4) According to the size of steel frame in this paper, the vertical correlation of fluctuating wind load cannot be ignored. However, only one degree of freedom (horizontal) is considered in this paper. Hope the author can consider this factor.	The authors agree with the reviewer's comments. Wind can cause simultaneous horizontal loadings and vertical loadings on the structure. For tall structures and flexible structures, the vertical stiffness is much larger in comparison to the horizontal stiffness and thus the vertical loads exert only a minimal effect on the vertical axis force on the structure. In such cases, the wind loadings in the calculation can be assumed to be horizontal actions. However, the vertical loads of wind greatly affect the vibration of space structures and long-span structures, and thus should be taken into consideration in the design process. In the tested steel framed structure used in this study, the column-beam connections were built as hinge joints with three parallel springs to facilitate rotation. The steel framed structure was therefore flexible in the horizontal direction. Thus, the wind loads were simplified as horizontal actions. Furthermore, due to the single-degree-of-freedom limitation of the shaking table in the laboratory, the wind loads can only be excited horizontally. For civil engineering applications, both horizontal and vertical wind loadings should be considered in the analytical model to ensure an accurate design. The explanation above has been included in the final paragraph of Section 5.4.
(5) When the remarkable period of wind load is close to the natural vibration period of the building structure, the wind-induced vibration will not only cause the structure damage, but also cause the residents' discomfort. Then, whether the ground motion input in this paper takes this special	The authors agree with the special case raised by the reviewer, and it is true that the vibration amplitude could be substantially greater when the frequencies of the wind and the structure become equal. This is because the resonance between loading frequency and structural frequency can cause enormous vibration. The SMA-based TMD is

case into account. I hope the author can explain.	designed to reduce the risk of this special case occurring. The explanation was presented in our published feasibility study: HUANG, H., CHANG, W. -S. & MOSALAM, K. M. 2017. Feasibility of shape memory alloy in a tuneable mass damper to reduce excessive in-service vibration. Structural Control & Health Monitoring, 24, 1-14. The following figure (cited by Huang et al. (2017)) shows the results of our TMD tests. The blue curve denotes the vibration amplitude of the main structure without TMD control. At frequencies of around 4-5 Hz, the amplitude is extremely large, a result attributable to the resonance between loading frequency and structural frequency. The orange curve shows the reduction in vibration amplitude that occurs when employing a SMA-based TMD. The vibration can clearly be reduced in a wider frequency band. 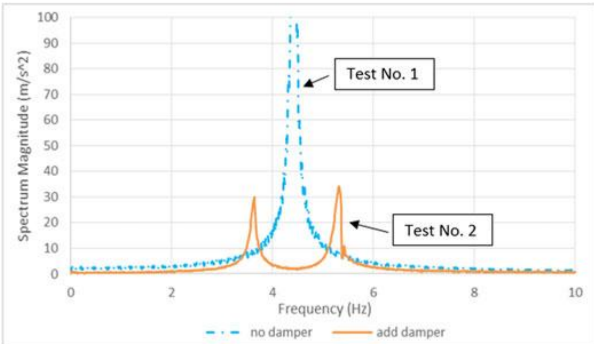 In a future extension of this study, one single SMA-based TMD can be replaced by SMA-based multi-TMD (MTMD) system. MTMD means that more than one TMD is installed on the structure in parallel or in series (Nigdeli and Bekdas, 2019, Arfiadi, 2016). MTMD can distribute natural frequency and can be designed to tune several modes of structural vibration. Consequently, the vibration amplitude can be reduced further in a wider frequency range. The discussion above has been included in the fourth paragraph in Section 5.4 and is marked in red.

Reviewer #1:

Reviewer's comments	Response to reviewer
(1) In introduction, there are no dates for Connor et al. It must be the following study. Connor, J., & Laflamme, S. (2014). Structural motion engineering (Vol. 476). New York: Springer. So. Give it as Connor and Laflamme (2014) and correct it in references.	The authors thank the reviewers for their efforts in correcting the references. The in-text citation and the corresponding reference have now been corrected.
(2) In the paper, the optimum tuning method of Warburton was used. Why this method is choosen? The other methods must be also mentioned. In future studies, I suggest to use other methods, espacially the curve fitting formulations given in Yucel et al. 2019. Yucel, M., Bekdaş, G., Nigdeli, S. M., & Sevgen, S. (2019). Estimation of optimum tuned mass damper parameters via machine learning. Journal of Building Engineering, 26, 100847.	There are two reasons why the Warburton (1982) method was selected as the optimal design method in this study. Firstly, the Warburton method is a classical analytical procedure for designing optimum parameters of TMD under various combinations of excitation and response, which is suitable for the civil engineering application employed in this study. The Warburton method has been widely cited and its effectiveness was demonstrated in previous studies by Hadi and Arfiadi (1998), Miguel et al. (2016) and Islam et al. (2018). Secondly, the Warburton method is a simplified analytical procedure and thus the semi-active vibration control in this study can be eased. The explanation above has been included in the second paragraph in Section 2.2 and is marked in red. The authors thank the reviewer for their recommendation. Machine learning provides a more effective analytical method for the optimal design of TMD parameters. The authors will strongly consider using the method proposed by Yucel et al. (2019), which has been cited in the fifth paragraph of Section 5.4.
I suggest mentioning the following studies. Yucel, M., Bekdaş, G., Nigdeli, S. M., & Sevgen, S. (2019). Estimation of optimum tuned mass damper parameters via machine learning. Journal of Building Engineering, 26, 100847. Leung, A.Y.T., Zhang, H., 2009, Particle swarm optimization of tuned mass dampers, Engineering structures, 31 (3), 715-728. Pourzeynali, S., Salimi, S., Kalesar, H. E., 2013, Robust multi-objective optimization design of tmd control device to reduce tall building responses against earthquake excitations using genetic algorithms, Scientia iranica, 20 (2), 207-221.	The authors thank the reviewer for recommending studies on the optimal design of TMD. We have cited all the studies suggested in the fourth and fifth paragraphs of Section 5.4. A discussion on the optimal design of TMD has been included in the fifth paragraph and is marked in red. This reads as follows: "The optimal TMD design method used in this study is the Warburton method (Warburton, 1982), because this study was conducted on a laboratory scale. More precise and effective optimal design methods are required by the full-scale SMA-based tuned mass damper to control large-size structures. Bekdaş and Nigdeli (2011), Nigdeli and Bekdas (2013), Bekdaş et al. (2017),

Arfiadi, Y., 2016, Reducing response of structures by using optimum composite tuned mass dampers, Procedia engineering, 161, 67-72. Farshidianfar, A., Soheili, S. 2013, ABC optimization of tmd parameters for tall buildings with soil structure interaction, Interaction and multiscale mechanics, 6 (4), 339-356. Bekdaş G, Nigdeli SM, Yang X-S, Metaheuristic Based Optimization for Tuned Mass Dampers Using Frequency Domain Responses. In: Harmony Search Algorithm. Advances in Intelligent Systems and Computing, vol 514, Del Ser J. (eds) Springer, pp. 271-279, 2017. Bekdaş, G., & Nigdeli, S. M. (2011). Estimating optimum parameters of tuned mass dampers using harmony search. Engineering Structures, 33(9), 2716-2723. Nigdeli, S.M. and Bekdaş, G. (2017), "Optimum tuned mass damper design in frequency domain for structures", KSCE Journal of Civil Engineering, 21(3), 912-922. Nigdeli, S. M., & Bekdas, G. (2014). Optimum tuned mass damper approaches for adjacent structures. Earthquakes and Structures, 7(6), 1071-1091. Bekdaş G., Nigdeli SM, Yang X-S. A novel bat algorithm based optimum tuning of mass dampers for improving the seismic safety of structures. Engineering Structures 2018; 159: 89-98. Nigdeli, S. M., & Bekdaş, G. (2019). Optimum design of multiple positioned tuned mass dampers for structures constrained with axial force capacity. The Structural Design of Tall and Special Buildings, e1593. Bekdaş, G., Kayabekir, A. E., Nigdeli, S. M., & Toklu, Y. C. (2019). Transfer function amplitude minimization for structures with tuned mass dampers considering soil-structure interaction. Soil Dynamics and Earthquake Engineering, 116, 552-562. Nigdeli, S. M., & Bekdas, G. (2013). Optimum tuned mass damper design for preventing brittle fracture of RC buildings. Smart Structures and Systems, 12(2), 137-155.	and Nigdeli and Bekdaş (2017) have developed optimal design methods employing the harmony search algorithm. Optimal design methods employing novel algorithms such as Particle swarm optimisation algorithm (Leung and Zhang, 2009) and machine learning algorithm (Yucel et al., 2019) have recently developed and can be incorporated into the SMA-based TMD to increase the tuning efficiency in future research. Structures not only sustain wind loads; they also suffer seismic loads. Therefore, a reduction in seismic vibration should be taken into consideration in the optimal design procedures employed in further studies of SMA-based TMD (Pourzeynali et al., 2013, Farshidianfar and Soheilia, 2013, Nigdeli and Bekdas, 2014, Bekdaş et al., 2018, Bekdaş et al., 2019).“

***Conflict of Interest Form**

We wish to draw the attention of the Editor to the following facts which may be considered as potential conflicts of interest and to significant financial contributions to this work.   [OR] We wish to confirm that there are no known conflicts of interest associated with this publication and there has been no significant financial support for this work that could have influenced its outcome.

We confirm that the manuscript has been read and approved by all named authors and that there are no other persons who satisfied the criteria for authorship but are not listed. We further confirm that the order of authors listed in the manuscript has been approved by all of us.

We confirm that we have given due consideration to the protection of intellectual property associated with this work and that there are no impediments to publication, including the timing of publication, with respect to intellectual property. In so doing we confirm that we have followed the regulations of our institutions concerning intellectual property.

We understand that the Corresponding Author is the sole contact for the Editorial process (including Editorial Manager and direct communications with the office). He/she is responsible for communicating with the other authors about progress, submissions of revisions and final approval of proofs. We confirm that we have provided a current, correct email address which is accessible by the Corresponding Author and which has been configured to accept email from w.chang@sheffield.ac.uk

Signed by all authors as follows:

Haoyu Huang

Wen-Shao Chang

***Declaration of Interest Statement**

Declaration of interests

☒ The authors declare that they have no known competing financial interests or personal relationships that could have appeared to influence the work reported in this paper.

☐The authors declare the following financial interests/personal relationships which may be considered as potential competing interests: